

# Cascade of field-induced magnetic transitions in a frustrated antiferromagnetic metal-possible experimental signature of a magnetic supersolid phase

A. I. Coldea,<sup>1,2,\*</sup> L. Seabra,<sup>3,4,2</sup> A. McCollam,<sup>5</sup> A. Carrington,<sup>2</sup> L. Malone,<sup>2</sup> A. F. Bangura,<sup>6,7,2</sup> D. Vignolles,<sup>8</sup> P. G. van Rhee,<sup>5</sup> R. D. McDonald,<sup>9</sup> T. Sörgel,<sup>6</sup> M. Jansen,<sup>6</sup> N. Shannon,<sup>10,1,2</sup> and R. Coldea<sup>1,2</sup>

<sup>1</sup>Clarendon Laboratory, Department of Physics, University of Oxford, Parks Road, Oxford OX1 3PU, U.K.

<sup>2</sup>H. H. Wills Physics Laboratory, University of Bristol, Tyndall Avenue, BS8 1TL, United Kingdom

<sup>3</sup>Department of Physics, Technion — Israel Institute of Technology, Haifa 32000, Israel

<sup>4</sup>Max-Planck-Institut für Physik komplexer Systeme, 01187 Dresden, Germany

<sup>5</sup>High Field Magnet Laboratory, IMM, Radboud University Nijmegen, 6525 ED Nijmegen, The Netherlands

<sup>6</sup>Max-Planck-Institut für Festkörperforschung, Heisenbergstr. 1, 70569 Stuttgart, Germany

<sup>7</sup>RIKEN(The Institute of Physical and Chemical Research), Wako, Saitama 351-0198, Japan

<sup>8</sup>Laboratoire National des Champs Magnétiques Intenses (CNRS), Toulouse, France

<sup>9</sup>National High Magnetic Field Laboratory, Los Alamos National Laboratory, MS E536, Los Alamos, New Mexico 87545, USA

<sup>10</sup>Okinawa Institute of Science and Technology, 1919-1 Tancha, Onna-son, Kunigami, Okinawa 904-0495, Japan

Frustrated magnets can exhibit many novel forms of order when exposed to high magnetic fields, however, much less is known about materials where frustration occurs in the presence of itinerant electrons. Here we report thermodynamic and transport measurements on micron-sized single crystals of the triangular-lattice metallic antiferromagnet  $2H$ -AgNiO<sub>2</sub>, in magnetic fields of up to 90 T and temperatures down to 0.35 K. We observe a cascade of magnetic phase transitions at 13.5, 20, 28 and 39 T in fields applied along the easy axis, and we combine magnetic torque, specific heat and transport data to construct the field-temperature phase diagram. The results are discussed in the context of a frustrated easy-axis Heisenberg model for the localized moments where intermediate applied magnetic fields are predicted to stabilize a magnetic supersolid phase. Deviations in the measured phase diagram from this model predictions are attributed to the role played by the itinerant electrons.

Frustrated magnets have proved a rich source of novel magnetic ground states such as spin liquids on triangular lattices and spin ices on pyrochlore lattices [1]. Another intriguing possibility, rooted in work on superfluid Helium, is that a frustrated magnet might realise a magnetic analogue of a supersolid, in which broken translational symmetry co-exists with a superfluid order parameter [2, 3]. Most experimental and theoretical studies of frustrated magnetism have focused on insulating systems, however, there are interesting examples of phenomena in metallic systems where frustration is believed to play a crucial role, such as heavy fermion physics in the spinel LiV<sub>2</sub>O<sub>4</sub> [4], and the metallic spin-liquid state in the pyrochlore Pr<sub>2</sub>Ir<sub>2</sub>O<sub>7</sub> [5]. In this context, the layered delafossites AgNiO<sub>2</sub> [6] and Ag<sub>2</sub>NiO<sub>2</sub> [7] provide model systems for studying the interplay of metallic electrons and local-moment magnetism on a geometrically-frustrated lattice.

Detailed structural studies on the hexagonal,  $2H$ -polytype, AgNiO<sub>2</sub> reveal a charge ordering transition at 365 K, below which one-third of the Ni ions form a triangular lattice of localized Ni<sup>2+</sup> ( $S = 1$ ) magnetic moments, while the remaining Ni<sup>3.5+</sup> ions form a honeycomb network of itinerant paramagnetic sites [8–11]. The localized Ni<sup>2+</sup> spins order magnetically below  $T_N = 19.5$  K into a collinear antiferromagnetic structure of alternating ferromagnetic stripes in the triangular plane, with spins aligned along the  $c$ -axis, while the itinerant Ni<sup>3.5+</sup> sites remain paramagnetic [8, 9]. Bandstructure calculations suggest that the Ag  $sp$  band is entirely above the Fermi level and that the structure can be visualized as a magnetic insulator formed by Ni<sup>2+</sup> (like NiO) with a strong tendency to magnetic order, superimposed on a Ni<sup>3.5+</sup> metal [8].

Here we report thermodynamic and transport measure-

ments on micron-size single crystals of  $2H$ -AgNiO<sub>2</sub> in high magnetic fields of up to 90 T applied along the  $c$ -axis. We observe a complex cascade of magnetic phase transitions, and combine magnetic torque, heat capacity and transport measurements to construct the field-temperature phase diagram. Experimental data are compared with the predictions of a frustrated easy-axis Heisenberg model for the localized Ni<sup>2+</sup> moments, which predicts a field-driven phase transition from the collinear antiferromagnet (CAF) into a magnetic supersolid (SS), which can be viewed as a Bose condensate of magnons of the CAF phase. Deviations from this model compared to the measured phase diagram are attributed to the role played by the itinerant electrons.

For this study we use hexagonal-shaped single crystals (typical size  $\sim 70 \times 70 \times 0.1 \mu\text{m}^3$ ) grown under high oxygen pressure [6]. We performed a series of torque measurements (on more than 10 single crystals) using piezo-resistive, self sensing cantilevers, at low temperatures (0.3 K) both in static magnetic fields (up to 18 T in Oxford and Bristol, 33 T at the HMFL in Nijmegen) and in pulsed fields (up to 55 T at the LNCMP, Toulouse and up to 90 T at NHMFL in Los Alamos). The longitudinal magnetisation was measured by force magnetometry using a highly sensitive magnetometer developed in Nijmegen [12]. Specific heat was measured using a purpose built micro-calorimeter using dc and relaxation techniques. The residual resistivity ratio is up to  $\sim 250$ , which indicates the high purity of the single crystals.

Magnetic torque in magnetic materials is caused by anisotropy, measuring the misalignment of the magnetization with respect to an uniform applied field. The torque exerted on a sample in an applied magnetic field  $\mathbf{H}$  is  $\tau = \mathbf{M} \times \mu_0 \mathbf{H}$

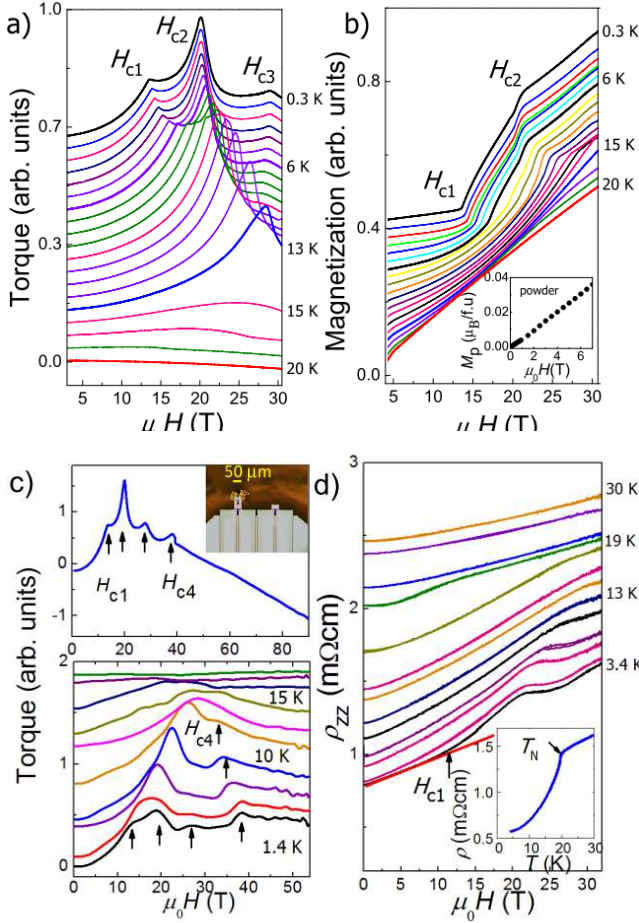


FIG. 1. (color online) High magnetic field measurements of micron-size single crystals of 2H-AgNiO<sub>2</sub>. Field dependence of (a) torque, and (b) magnetization at constant temperature  $T$  for field  $\mathbf{H}$  nearly along the  $c$ -axis ( $\theta \approx 3^\circ$ ). The inset shows magnetization data for a powder sample at 5 K. c) Torque data up to 90 T measured at constant temperatures in pulsed magnetic fields on two different samples (top and bottom panels). Magnetic transitions are indicated by arrows and labels. Top inset shows a typical crystal mounted on a piezolever. d) Field dependence of interlayer transport at constant temperatures below 30 K when  $\mathbf{H} \parallel c$  (within  $\theta \approx 3^\circ$ ). The arrow indicates the deviation from the linear dependence at  $H_{c1}$ . The inset shows the low-temperature resistivity and the arrow indicates the position of the magnetic ordering transition at  $T_N = 19.5$  K. In all panels traces at different temperatures are uniformly shifted vertically for clarity.

where  $\mathbf{M}$  is the bulk magnetization. If  $\mathbf{M}$  and  $\mathbf{H}$  lie in the  $(ac)$  plane, then  $\tau = \mu_0(M_a H_c - M_c H_a) = \frac{1}{2}\mu_0(\chi_a - \chi_c)H^2 \sin 2\theta$ , with  $\theta = 0$  when  $\mathbf{H} \parallel c$ . Thus, torque experiments measure the anisotropy of the magnetization in the  $ac$  plane and the torque vanishes in field along the  $c$ - and  $a$ -axes (when  $\sin 2\theta = 0$ ); the longitudinal magnetization provides access to the parallel  $M_c$  component of the sample magnetization.

Figs. 1(a) and (b) show the field and temperature dependence of the torque and magnetization respectively, performed with the magnetic field aligned close to the easy axis  $c$ . At low temperatures and in low magnetic fields, the torque signal varies as  $\tau \sim H^2$  implying a constant anisotropy,  $\chi_a - \chi_c$ ,

in the CAF phase. By increasing the field, we observe kinks in torque at  $\mu_0 H_{c1-4} = 13.5, 20, 28$  and  $39$  T [see Figs. 1(a) and (c)], which we attribute to field-induced transitions. No further anomalies are detected at higher fields up to 90 T [see Fig. 1(c)], however the torque is finite and increases in absolute magnitude indicating that the magnetization is not yet saturated and the region above  $H_{c4}$  is most likely a phase with spontaneous magnetic order. Further evidence for the phase transitions seen in torque data is provided by magnetization measurements shown in Fig. 1(b). At low fields the magnetization has a weak linear field dependence and at  $H_{c1}$  the slope suddenly changes, suggesting a linear increase in the  $M_c$  component in this phase, followed by a decrease in slope above  $H_{c2}$  and a small kink at  $H_{c3}$ . Experiments of torque and specific heat in constant magnetic field as a function of temperature presented in Fig. 3(a) and (b) also show clearly the anomalies at  $T_N$  and  $T_{c1}$ . Later, we compare in detail these measurements with predictions for a spin Hamiltonian.

Another important fact about 2H-AgNiO<sub>2</sub> is that it is a good metal with low residual resistivity ( $57 \mu\Omega \text{ cm}$ ) (see Fig. 1(d)) and quantum oscillations have been observed [13]. There is a significant contributions to the density of states at the Fermi level originating from the Ni sites on the honeycomb lattice [8]. Fig. 1(d) shows that transport measurements also exhibit anomalies at the magnetic phase transitions, showing that the itinerant  $d$  electrons are a sensitive probe of the magnetic ground state. There is a significant drop in resistivity below  $T_N$  (see inset in Fig. 1(d)), which is likely the result of suppression of electronic scattering by low-energy spin fluctuations when a spin gap opens below  $T_N$  [14]. Furthermore, magnetoresistance measurements in Fig. 1(d) indicate that in the vicinity of the magnetic transition there is a clear change in slope at  $H_{c1}$  that fades away with increasing temperature. In zero field the Ni<sup>2+</sup> spins order in a collinear antiferromagnetic pattern with spins pointing along the easy  $c$ -axis, schematically shown in Fig. 2(c) [8, 14]. In magnetic fields applied along the easy axis a transition is expected in a field of  $\Delta/(g\mu_B)$  that matches the zero-field anisotropy spin gap,  $\Delta$ . Using the observed value of the first transition field  $\mu_0 H_{c1} = 13.5$  T in Fig. 1(a) gives  $\Delta = 1.57$  meV (using  $g = 2$ ), in good agreement with the value of  $1.7(1)$  meV estimated from inelastic neutron scattering measurements [14]. For easy-axis antiferromagnets with un-frustrated interactions the transition in field is to a spin-flop phase, signalled by an anomaly in torque [15–17]. This canted phase is then stable with increasing magnetic field, up to full magnetization saturation. However, for easy-axis triangular lattice antiferromagnets with frustrated interactions, as is believed to be the case for 2H-AgNiO<sub>2</sub>, an alternative scenario with a richer phase diagram has been proposed [23], which we describe below.

The magnetic field-temperature phase diagram of 2H-AgNiO<sub>2</sub>, based on magnetic torque, transport and specific heat data obtained over a large range of fields and temperatures on different single crystals, is shown in Fig. 2(a). Unexpectedly, in this metallic magnet, we observe a cascade of phase transitions suggesting the formation of different mag-

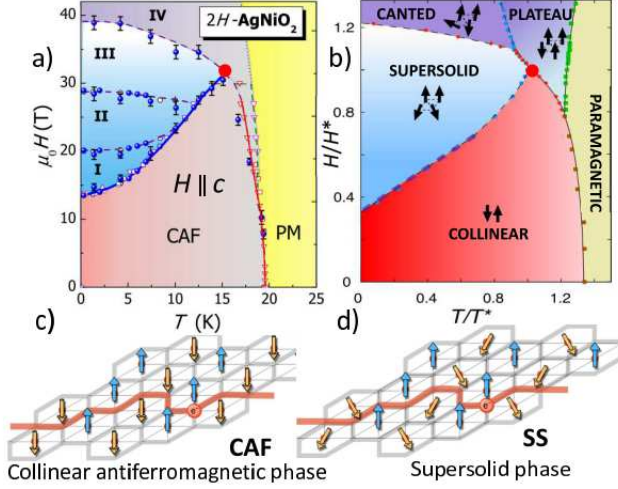


FIG. 2. (colour online) (a) The  $H - T$  phase diagram of  $2H\text{-AgNiO}_2$  from torque magnetometry (circles), specific heat (triangles) and transport (square). The solid and dashed lines indicate boundaries between different magnetic phases: collinear antiferromagnetic (CAF), field induced phases I-IV and paramagnetic (PM). (b) The phase diagram of the classical Heisenberg model on the triangular lattice with first- ( $J_1=1$ ) and second-neighbour ( $J_2=0.15$ ) in-plane interactions, coupling between layers ( $J_\perp=-0.15$ ) and easy-axis anisotropy  $D = 0.25$ , obtained from Monte Carlo simulation [24]. The axes units are scaled to the point (large solid red circle) where the CAF, SS and plateau phases meet with  $T^* = 0.3J_1$ ,  $B^* = 1.6J_1$ . In the CAF phase (c) the spin excitations are gapped, while in the SS phase (d) electrons can scatter from gapless spin excitations.

netic structures with increasing magnetic field, different from typical uniaxial antiferromagnets, see e.g. Refs. [15, 18–20]. In insulators, field-induced transitions were observed previously in two-dimensional  $\text{CuFeO}_2$  ( $S = 5/2$ ), with a related delafossite-type structure [21], and extended models were developed for  $S = 1$  [22].

To gain insight into the magnetism of  $2H\text{-AgNiO}_2$  in high magnetic fields, we consider a simple effective spin model describing only the localised  $S = 1$  ( $\text{Ni}^{2+}$ ) spins interacting via a Heisenberg model including first- and second-neighbour antiferromagnetic exchange ( $J_1, J_2$ ) on the triangular lattice, a coupling between layers ( $J_\perp$ ) and easy-axis anisotropy ( $D$ ), using parameters obtained from fits to powder inelastic neutron scattering data [14]. The resulting magnetic phase diagram in easy-axis field obtained from classical Monte Carlo simulations was described in detail in Refs. [23, 24] and in the Supplementary Material. Here, we focus on the low-field region of the phase diagram of the spin model in Fig.2(b), and we compare directly the measured and the calculated thermodynamic quantities: torque, magnetization and specific heat.

The experimental phase diagram in Fig. 2(a) shows that the phase boundary between the CAF phase and phase I have an unusual field-temperature dependence, i.e. the transition field  $H_{c1}$  increases strongly with increasing temperature. This behavior is well reproduced by the theoretical phase diagram in

Fig. 2(b), there the phase transition CAF-SS is understood in terms of Bose-Einstein condensation of magnons within the CAF state [23]; this converts the two-sublattice CAF order into an unusual four-sublattice state, in which two sublattices have spins “up” and the other two have spins “down” and canted away from the easy axis, as illustrated in Fig. 2(d). These canted spin components break spin-rotation symmetry about the magnetic field, and behave like a superfluid order parameter. Meanwhile the components of spin along the magnetic easy axis break the discrete translational symmetry of the lattice, in a way analogous to a solid, therefore, the resulting state is a *magnetic supersolid* [23, 24].

Next, we compare directly the experimental results for magnetic torque, magnetization and specific heat with those predicted by The temperature-dependence of the torque at fixed field has a very similar shape and qualitative form between in the experiment and theoretical model [see Fig. 3(a) and (b)]: in both cases upon cooling from high temperatures in the paramagnetic phase the torque changes sign below  $T_N$ , increases upon decreasing temperature in the CAF phase, then has a peak at  $T_{c1}$ , identified with the transition into the SS phase. The temperature-dependence of the specific heat data in constant magnetic fields also shows consistent behavior between experiment and theory, see Fig. 3(c) and (d). At low fields a single anomaly is observed at the  $T_N$  transition. In fields above  $H_{c1}$  a second anomaly is observed at low temperatures  $T_{c1}$  identified with the transition CAF-SS and this shifts to higher temperatures upon increasing field [25]. At those higher fields an additional anomaly (labelled as  $T'$ ) appears near  $T_N$ , this feature is also present in the theoretical model, where it is associated with the transition to another intermediate-temperature phase (labelled “plateau” in Fig.2(b)).

Following the same approach, we discuss the measured field dependencies of magnetic torque and magnetisation at constant temperature, shown in Fig. 1(a,b), with those predicted by the model in Fig. 3(e,f). At very low temperatures in the CAF phase, the measured and simulated magnetization are both linear in  $H$ , whereas the torque shows a quadratic dependence,  $H^2$ , as a function of magnetic field, and displays a kink at the first critical field,  $H_{c1}$ , that becomes sharper upon lowering temperature. Furthermore, inside the SS phase at fields right above the transition  $H_{c1}$ , magnetic torque is observed to be almost independent of the applied field (see Fig.3(e)). All these observations are at odds with standard spin-flop transitions, see Refs. [15–17, 19, 20]; in those cases, torque should show a strong divergence at a spin-flop transition field  $H_c$ , then becomes strongly suppressed above  $H_c$ , whereas the magnetization would have an abrupt jump at  $H_c$ , indicative of the first-order nature of this transition. The transition field for a spin-flop transition is usually independent of temperature, since it is determined by a balance of energies between different spin configurations rather than entropy.

While the classical spin model for the localized  $\text{Ni}^{2+}$  moments can provide a good description of many of the qualitative and quantitative features of the lowest field-induced tran-



sition observed at  $H_{c1}$ , the model cannot capture the full phase diagram and in particular cannot account for the presence of multiple phases spanning relatively narrow field ranges above  $H_{c1}$  (labelled as I-III). It may be possible that itinerant elec-

trons, neglected in the spin model, could affect the phase diagram in this region of intermediate fields and potentially lead to additional transitions at  $H_{c2}$  and  $H_{c3}$  inside the SS phase of the classical model. In the SS phase the broken translational symmetry of the *solid* may lead to reconstruction of the Fermi surface, while the gapless Goldstone modes of the *superfluid* may lead to the inelastic scattering of electrons and thus an increase of resistivity above  $H_{c1}$ , as observed in Fig. 1(d). A possible reconstruction of the Fermi surface at the low-field transition may also explain why more entropy is released in experiment than in theory at the SS transition, indicated by the large anomaly in specific heat at  $T_{c1}$  in Fig. 3(c) and (d).

The observed  $H - T$  phase diagram of  $2H\text{-AgNiO}_2$  reflects the complexity of its magnetic interactions. Since localized magnetic moments are embedded in a metal, they are subject to RKKY interactions, which, unlike superexchange, decays slowly with distance and may provide non-negligible further-neighbour exchange. Furthermore, the band structure calculations show a small, but finite magnetic moment ( $m_i \approx 0.1 - 0.2\mu_B$ ) [8] on the itinerant and inherently non-magnetic Ni sites on the honeycomb (see Fig. 2c). The Hund's rule coupling on these sites may provide an additional incentive for the localized spins to order and the scale of this interaction given by  $Im_i^2/4$  is a few meV (the Stoner factor is  $I \approx 0.6 - 0.8$  eV). By a similar mechanism, the Hund's energy of induced moments generates ferromagnetism in  $\text{SrRuO}_3$  [26].

In conclusion, we have probed the magnetic phase diagram of the frustrated antiferromagnetic metal,  $2H\text{-AgNiO}_2$ , in strong magnetic fields applied along the easy axis and have observed a cascade of magnetic phase transitions. Thermodynamic measurements have been compared with predictions of an effective localized spin model, which explains part of the phase diagram and identifies a novel magnetic supersolid phase. However, a more realistic model for  $2H\text{-AgNiO}_2$  needs to consider also the itinerant  $d$  electrons on the honeycomb lattice, which may participate in the exchange interactions and may affect the magnetic order of the localized moments. Therefore, the itinerant electrons may be responsible for some of the higher-field transitions observed both in transport and thermodynamic measurements. Further studies will explore how those phase transitions correlate with changes of the Fermi surface topology in this frustrated magnetic metal where  $d$  electrons have mixed localized and itinerant character.

We acknowledge and thank J. Analytis, C. Jaudet, P.A. Goddard, Jos Perenboom, M.D. Watson, for technical support during experiments. We thank I.I. Mazin, A. Schofield, I. Vekhter for useful discussions. This work was supported by EPSRC Grants EP/I004475/1, EP/C539974/1, EP/G031460/1, FCT Grant No. SFRH/BD/27862/2006, and the EuroMagNET II (EU Contract No. 228043). AIC acknowledges an EPSRC Career Acceleration Fellowship (EP/I004475/1). RMcd acknowledges support from BES "Science of 100 T".

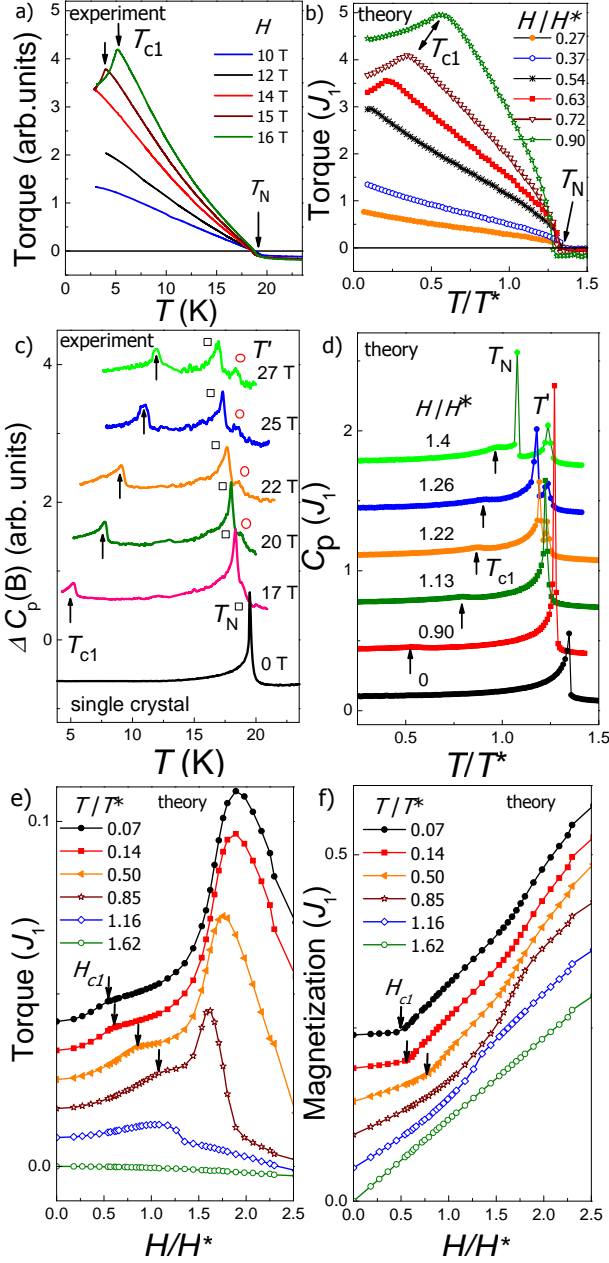


FIG. 3. (color online) Temperature-dependence of torque at fixed applied field in (a) experiments and (b) theoretical model. Temperature-dependence of specific heat at fixed field in (c) experiment and (d) theory. Identified transitions are indicated by arrows at  $T_{c1}$ , squares at  $T_N$  and circles at  $T'$ . Calculated (e) torque and (f) magnetisation as a function of applied field at constant temperatures compared with experimental data in Fig. 1(a), (b) ( $\theta = 5^\circ$ ). In the theoretical model saturation occurs for  $H/H^* \approx 4.8$  with  $T^*$  and  $H^*$  defined in Fig 2(b). Traces at different fields (c,d) and different temperatures (e,f) are shifted vertically for clarity.

---

\* corresponding author: amalia.coldea@physics.ox.ac.uk

- [1] For a review see L. Balents, *Nature* **464**, 199 (2010).
- [2] H. Matsuda and T. Tsuneto, *Prog. Theor. Phys. Suppl.* **46**, 411 (1970).
- [3] K.S. Liu and M.E. Fisher, *J. Low Temp. Phys.* **10**, 655 (1973).
- [4] C. Urano, M. Nohara, S. Kondo, F. Sakai, H. Takagi, T. Shiraki and T. Okubo, *Phys. Rev. Lett.*, **85** 1052 (2000).
- [5] S. Nakatsuji, Y. Machida, Y. Maeno, T. Tayama, T. Sakakibara, J. van Duijn, L. Balicas, J.N. Millican, R.T. Macaluso and J. Y. Chan, *Phys. Rev. Lett.* **96**, 087204 (2006).
- [6] T. Sörgel and M. Jansen, *Z. Anorg. Allg. Chem.* **631** 2970 (2005).
- [7] H. Yoshida, Y. Muraoka, T. Sörgel, M. Jansen and Z. Hiroi, *Phys. Rev. B* **73**, 020408 (2006).
- [8] E. Wawrzynska, R. Coldea, E. M. Wheeler, I. I. Mazin, M. D. Johannes, T. Sörgel, M. Jansen, R. M. Ibberson, and P. G. Radaelli *Phys. Rev. Lett.* **99**, 157204 (2007).
- [9] E. Wawrzynska, R. Coldea, E. M. Wheeler, T. Sörgel, M. Jansen, R. M. Ibberson, and P. G. Radaelli, M. M. Koza, *Phys. Rev. B* **77**, 094439 (2008).
- [10] I. I. Mazin, D. I. Khomskii, R. Lengsdorf, J. A. Alonso, W. G. Marshall, R. M. Ibberson, A. Podlesnyak, M. J. Martinez-Lope, and M. M. Abd-Elmeguid, *Phys. Rev. Lett.* **98**, 176406 (2007).
- [11] G. L. Pascut, R. Coldea, P. G. Radaelli, A. Bombardi, G. Beutier, I. I. Mazin, M. D. Johannes, and M. Jansen *Phys. Rev. Lett.* **106**, 157206 (2011).
- [12] A. McCollam, P. G. van Rhee, J. Rook, E. Kampert, U. Zeitler, and J. C. Maan *Rev. Sci. Instrum.* **82**, 053909 (2011).
- [13] A.I. Coldea, in preparation (2014).
- [14] E. M. Wheeler, R. Coldea, E. Wawrzynska, T. Sörgel, M. Jansen, M. M. Koza, J. Taylor, P. Adroguer, and N. Shannon *Phys. Rev. B* **79**, 104421 (2009).
- [15] H. Uozaki, T. Sasaki, S. Endo, and N. Toyota, *Journal of the Physical Society of Japan* **69**, 2759 (2000).
- [16] T. Nagamiya, K. Yosida, and R. Kubo, *Advances in Physics* **4**, 1 (1955).
- [17] A. N. Bogdanov, A. V. Zhuravlev, and U. K. Rößler, *Phys. Rev. B* **75**, 094425 (2007).
- [18] T. Kawamoto, Y. Bando, T. Mori, T. Konoike, Y. Takahide, T. Terashima, S. Uji, K. Takimiya, T. Otsubo, *Phys. Rev. B* **77**, 224506 (2008).
- [19] C. C. Becerra, N. F. Oliveira, A. Paduan-Filho, W. Figueiredo, and M. V. P. Souza, *Phys. Rev. B* **38**, 6887 (1988).
- [20] R. Toft-Petersen, N. H. Andersen, H. L., J. Li, W. Tian, S. L. Bud'ko, T. B. S. Jensen, C. Niedermayer, M. Laver, O. Zaharko, J. W. Lynn, and D. Vaknin, *Phys. Rev. B* **85**, 224415 (2012).
- [21] N. Terada Y. Narumi, Y. Sawai, K. Katsumata, U. Staub, Y. Tanaka, A. Kikkawa, T. Fukui, K. Kindo, T. Yamamoto, R. Kanmuri, M. Hagiwara, H. Toyokawa, T. Ishikawa, and H. Kitamura, *Phys. Rev. B* **75**, 224411 (2007).
- [22] P. Sengupta and C. D. Batista, *Phys. Rev. Lett.* **99**, 217205 (2007).
- [23] L. Seabra and N. Shannon *Phys. Rev. Lett.* **104**, 237205 (2010).
- [24] L. Seabra and N. Shannon *Phys. Rev. B* **83**, 134412 (2011).
- [25] In the limit of our experimental resolution (specific heat experiments are performed on extremely small samples) as a function of temperature (experiments were made on  $70 \times 70 \times 10 \mu\text{m}^3$  crystals) we cannot detect clear signatures for the other two transitions clearly observed both in the torque and transport measurements. This could be due to the fact that the scans were performed mainly at constant temperature and transition bound-

aries are nearly flat and/or that these transitions are related to a reorientation of spins which does not imply a significant change in energy and do not result in a large anomaly in the specific heat.

- [26] I.I. Mazin and D.J. Singh, *Phys. Rev. B*, **56** 2256 (1997).